Inorganic Chemistry

Article

pubs.acs.org/IC

Unexpected Formation of Chiral Pincer CNN Nickel Complexes with β-Diketiminato Type Ligands via C−H Activation: Synthesis, Properties, Structures, and Computational Studies

Zhengliang Lu,[†,§] Srinivas Abbina,[†] Jared R. Sabin,[‡] Victor N. Nemykin,*[,‡] and Guodong Du*[,†]

[†]Department of Chemistry, University of North Dakota, 151 Cornell Street Stop 9024, Grand Forks, North Dakota 58202, United States

[‡]Department of Chemistry & Biochemistry, University of Minnesota Duluth, 1039 University Drive, Duluth, Minnesota 55812, United States

Supporting Information

ABSTRACT: Reaction of lithiated chiral, unsymmetric β-diketimine type ligands $\mathbf{HL}^{2a-e}$ containing oxazoline moiety ($\mathbf{HL}^{2a-e}$ = 2-(2′-R_1NH)-phenyl-4-R_2-oxazoline) with *trans*-NiCl(Ph)$(PPh_3)_2$ afforded a series of new chiral CNN pincer type nickel complexes (**3a−3e**) via an unexpected cyclometalation at benzylic or aryl C−H positions. Single crystal X-ray diffraction analysis established the pincer coordination mode and the strained conformation. Chirality, and in one case, racemization of the target nickel complexes were confirmed by circular dichroism (CD) spectroscopy. Electronic structure and band assignments in experimental UV−vis and CD spectra were discussed on the basis of Density Functional Theory (DFT) and time-dependent (TD) DFT calculations.

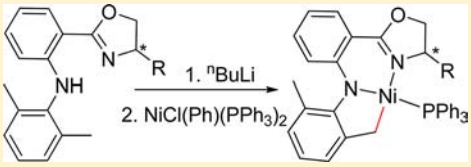

INTRODUCTION

Ligands play an essential role in catalysis, especially when regio, stereo, and enantioselectivities are concerned, as they can provide appropriate stereochemical and electronic environments around the active metal centers. Among the various chelating ligands available in the literature, tridentate pincer ligands are one of the most widely applied systems.[1] The prototypical DXD-type pincer ligands feature two donor atoms (D) such as tertiary phosphine or amine linked through an aromatic or aliphatic skeleton encompassing a carbon- or nitrogen-bound anionic anchor (X) (Chart 1). In particular,

Chart 1. General Representation of Pincer Ligands

D, D′ = N, P, S, O, C, etc

X = C, N, P, Si, B, etc

NCN and PCP pincer complexes with overall C_2 symmetry are widespread, and this design, with the carbon−metal bond located between two lateral arms, leads to stabilization of the C-M bond and could improve the robustness of catalytic systems.[2] It is also important that such framework can be fine-tuned to allow rational design of catalysts. Variations of donor and anchor atoms have greatly expanded the range of pincer ligands, in which D can be N, P, S, O, C, etc., and X can be C, Si, N, P, B, etc.[1,3]

Among these variations, the unsymmetric pincer ligands of the DXD′ type have received increasing attention.[4,5] The two donor groups (D and D′) can be markedly different, which may result in unique and novel properties in the pincer complexes. Transition metal complexes based on the CNN pincer have been synthesized and employed in the catalytic cross coupling,[6] hydrogenation of esters,[5a] and transfer hydrogenation of ketones.[7] The carbon donors in these systems are typically based on aryl (**1a−b**) or N-heterocyclic carbene (**1c−f**) carbons (Chart 2). The introduction of chiral substituents in the pincer framework constitutes a common strategy for enantioselective catalysis.[8,9] However, pincer complexes with both unsymmetric and chiral ligands have been relatively less developed,[10] presumably because of lack of a general synthetic strategy, and only a few complexes incorporating chiral CNN pincer ligands, derived from **1a** and **1e**, have been reported.[11]

Nickel is one of the first metals incorporated in the pincer complexes,[12] and numerous pincer nickel complexes have appeared in the literature.[13] Their applications in bond activation and catalysis such as C−C coupling, dehydrogenation, and hydroamination have been extensively studied.[6a,b,14,15] The potential exhibited by these complexes has encouraged further development of ligand precursors bearing analogous chelating systems and isoelectronic features.[16] In this report we describe the synthesis and characterization of a series of rare chiral CNN pincer nickel complexes with C_1-symmetry β-diketiminato type ligands, in which the carbon donor arm is formed via an intramolecular

Received: October 8, 2012
Published: January 15, 2013

   dx.doi.org/10.1021/ic3021904 | *Inorg. Chem.* 2013, 52, 1454−1465

Chart 2. Some Examples of CNN Pincer Ligands[a]

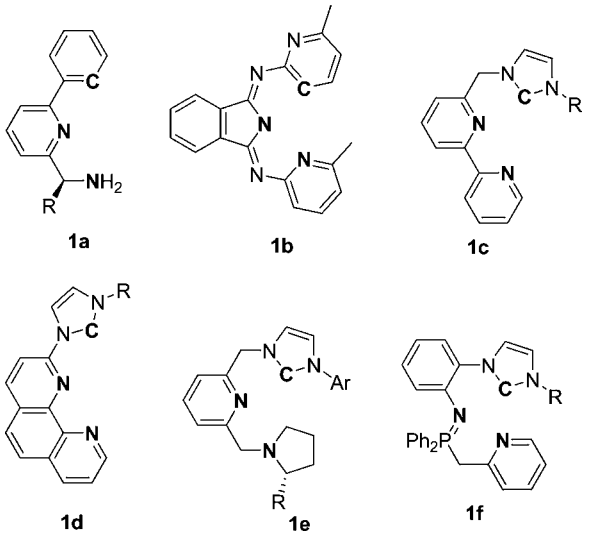

[a]Donor atoms are in bold.

C−H activation. Besides the unexpected C−H activation for both sp^3- and sp^2-hybridized carbon atoms, these complexes are of interest in catalysis given that the chiral ligand precursors are readily available and tunable. The C_1-symmetric systems have received increasing attention in recent years,[17] and the unsymmetric donor sets could be advantageous when two donor groups influence the reactivity and selectivity in different manners.[18] The presence of sp^3-C in the pincer framework may also lead to structural and electronic versatilities that can open up new opportunities in catalysis.[19]

RESULTS

Synthesis of Ligands. The chiral, unsymmetric anilido-imine ligands, **2a−e**, have been obtained as analogues of conventional β-diketiminato framework, via a palladium catalyzed Buchwald-Hartwig amination reaction (Scheme 1).[20] In the case of **2e**, because of the low and inconsistent yields, an alternative, Cu-catalyzed amination reaction protocol[21] was employed. This protocol seems to be more consistent and reliable for alkyl amines, although yields are still generally moderate (~40%).

Scheme 1. Synthesis of Ligands 2a−2e via Amination Reaction

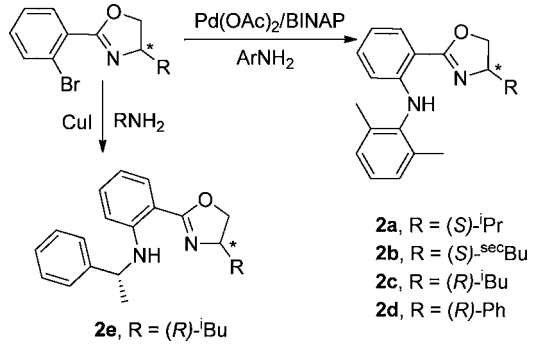

These ligands can be deprotonated with a strong base such as ^{n}BuLi at low temperature. Thus, the lithium salt of ligand **2d** was prepared by lithiation with stoichiometric amount of ^{n}BuLi and isolated as a yellow crystalline solid in good yields. The ^{1}H NMR indicates that the coordination environment of the lithium center is completed with two tetrahydrofuran (THF) solvent molecules. It was further noted that isolation of lithium salts was not necessary, and the subsequent metalation reactions were carried out using in situ generated lithium compounds without further purification.

Preparation of Pincer Nickel Complexes 3a−3d. Treatment of lithium salts of ligand **2a−d** with *trans*-$NiCl(Ph)(PPh_3)_2$ at room temperature resulted in an immediate color change, and dark-red crystals **3a−d** were consistently formed after allowing solutions standing for 2−5 days. The isolated compounds appeared rather sensitive to air, as the color blackened within minutes upon exposure to the air, but could be stored under an inert atmosphere for months. They are quite soluble in THF and toluene and have been characterized by various spectroscopic and analytic techniques including ^{1}H, ^{13}C, and ^{31}P NMR spectroscopy. In the ^{1}H NMR of **3a** in benzene-d_6 (Figure 1), the most striking features include the six-proton dimethyl group of the free ligands becoming a three-proton singlet, and the appearance of two new 1-proton multiplets at 2.76 and 1.38 ppm. The two multiplets are coupled with each other and connected to the same carbon atom, as indicated by 2D NMR analysis.[22] These observations suggest the metalation of one methyl group of the aniline moiety, leading to a coordinated methylene group ($NiCH_2$) with two diastereotopic protons riding on the same carbon (Scheme 2). Because of coupling with the phosphorus nuclei, the methylene protons are both multiplets, and this is further supported by a doublet of $NiCH_2$ at 26.43 ppm ($^2J_{C-P}$= 25.3 Hz) in the ^{13}C NMR.[23] The ^{1}H NMR spectra for **3b−d** reveal the similar features that coordinated methylene protons exhibit, two signals at 2.66 and 1.45 ppm for **3b**, 2.47 and 1.64 ppm for **3c**, and 2.48 and 1.56 ppm for **3d**, respectively; the $NiCH_2$ signals appear as doublets at 26.38 ppm for **3b**, 26.61 for **3c**, and 26.52 for **3d**, respectively, in ^{13}C NMR ($^2J_{C-P}$= 25.2 −26.5 Hz) due to coupling with the phosphorus nuclei.

The proposed structures of the Ni complexes were further verified by single-crystal X-ray diffraction experiments. The X-ray crystal data, data collection, and refinement parameters are summarized in Table 1. A single crystal X-ray structure of **3a** is presented in Figure 2. In agreement with the NMR data, one of the aniline methyl substituents is metalated with nickel, forming a five-membered metallacycle. This, along with the imine nitrogen atom, resulted in an unsymmetric, CNN pincer type coordination mode of the supposedly bidentate ligand. The triphenylphosphine ligand completed the distorted square-planar environment around nickel center. The Ni−P bond length of 2.1336(6) Å is in the typical range for similar compounds,[24] while the Ni−C bond distance of 1.930(2) Å is considerably shorter than the Ni−C(sp^3) bond (1.97 Å) in a PCP pincer complex,[25] but longer than the Ni−C(sp^2) bonds (1.88 Å) seen in the other pincer complexes.[26]

Complexes **3a−3c** are isomorphic with similar structural parameters; selected bond lengths and bond angles are listed in Table 2. The bond distances of Ni−N_{imino} (1.920−1.935 Å) are slightly longer than that of Ni−N_{amido} (1.908−1.920 Å), presumably because of the stronger interaction with anionic amido nitrogens. Both of them are in the normal range compared with other reported nickel compounds.[27] The coordination plane around nickel, however, appears to be severely distorted. While the N_{imino}−Ni−C bond angles of ~163° are not unusual for the trans angles involving the lateral

dx.doi.org/10.1021/ic3021904 | Inorg. Chem. 2013, 52, 1454−1465

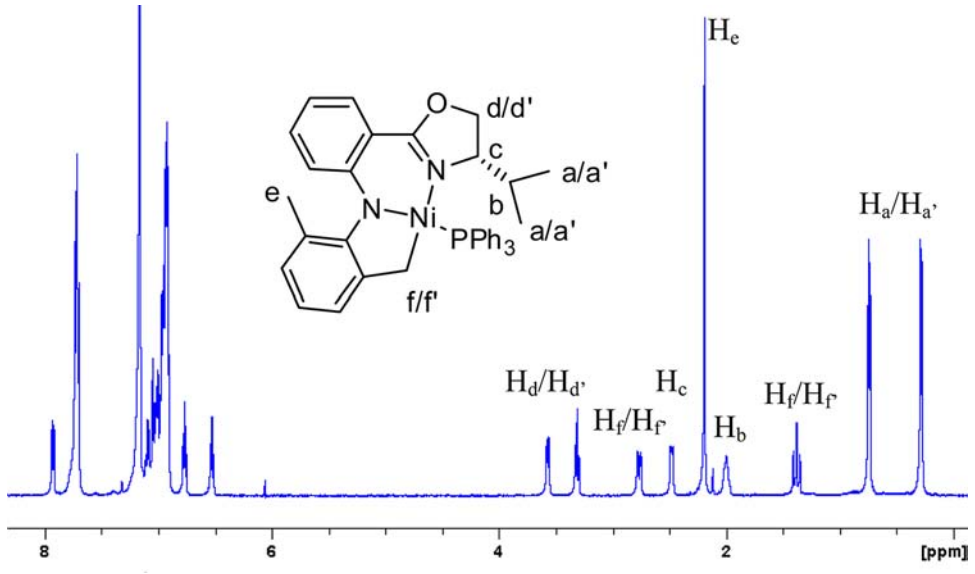

Figure 1. ^{1}H NMR of complex **3a** in C_6D_6 with partial assignment.

Scheme 2. Synthesis of Pincer Complexes 3a−d

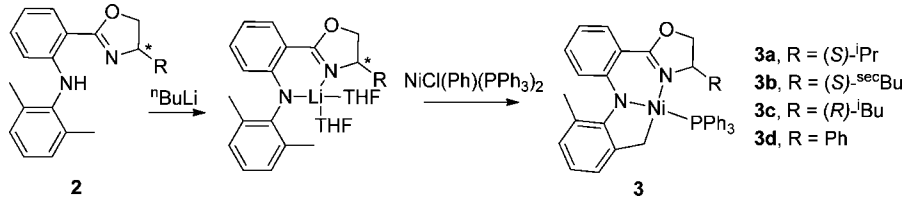

Table 1. X-ray Crystal Data, Data Collection Parameters, and Refinement Parameters

	3a	3b	3c	3d	3e	2d	4
formula	$C_{38}H_{37}N_2NiOP$	$C_{39}H_{39}N_2NiOP$	$C_{39}H_{39}N_2NiOP$	$C_{41}H_{35}N_2NiOP$	$C_{93}H_{84}ClLiN_2NiO_5P_4$	$C_{23}H_{22}N_2O$	$C_{75}H_{73}Ni_2P_5$
FW	627.41	641.43	641.43	661.39	1534.70	342.43	1366.74
crystal system	orthorhombic	orthorhombic	orthorhombic	triclinic	orthorhombic	orthorhombic	triclinic
space group	$P2_12_12_1$	$P2_12_12_1$	$P2_12_12_1$	$P\bar{1}$	$P2_12_12_1$	$P2_12_12_1$	$P\bar{1}$
a, Å	9.7830(2)	9.7903(2)	9.84280(10)	9.2807(2)	11.4071(3)	10.7615(11)	12.7404(4)
b, Å	15.0674(2)	15.3617(4)	15.0952(3)	11.2227(3)	20.7893(7)	10.8922(11)	12.8703(4)
c, Å	21.6014(15)	21.5085(15)	21.8779(15)	17.2906(4)	33.113(2)	15.7770(16)	24.2765(7)
α, deg				108.2600(10)			77.185(2)
β, deg				92.2040(10)			88.302(2)
γ, deg				103.0970(10)			61.962(2)
V, Å^3	3184.1(2)	3234.8(2)	3250.6(2)	1654.02(7)	7852.6(6)	1849.3(3)	3413.08(18)
Z	4	4	4	2	4	4	2
d_{calc}, g cm^{-3}	1.309	1.317	1.311	1.328	1.298	1.230	1.330
T/K	123	123	123	173	123	173	173
μ, mm^{-1}	0.692	0.683	0.680	0.670	0.418	0.076	0.716
2θ range, deg	3.118−27.484	3.111−27.482	3.094−27.484	1.25−33.09	3.003−24.710	2.29−28.22	0.86−28.30
data collected	22147	11925	23395	25654	32597	15880	86941
unique data	7309	7097	7369	10575	13331	4274	16805
R_{int}	0.025	0.036	0.021	0.0215	0.101	0.0249	0.1086
data in refinement	7294	7083	7355	10575	13292	4274	16805
data with $I > 2.0\sigma(I)$	6875	5413	6970	8835	8596	4021	9748
variables	389	398	398	415	965	237	813
$R(F_o)^a$	0.0246	0.0456	0.0276	0.0351	0.0596	0.0381	0.0561
$R_w(F_o^2)^b$	0.0438	0.0748	0.0553	0.0951	0.0818	0.1014	0.1373
GOF	0.9425	0.9724	0.9765	1.047	0.9568	1.038	0.933
Flack	−0.002(7)	−0.01(2)	0.004(9)		−0.036(16)		

$^a R = \sum||F_o| - |F_c||/\sum|F_o|$ for $F_o^2 > 2\sigma(F_o^2)$. $^b R_w = [\sum w(F_o^2 - F_c^2)^2/\sum w(F_o^2)^2]^{1/2}$.

dx.doi.org/10.1021/ic3021904 | Inorg. Chem. 2013, 52, 1454−1465

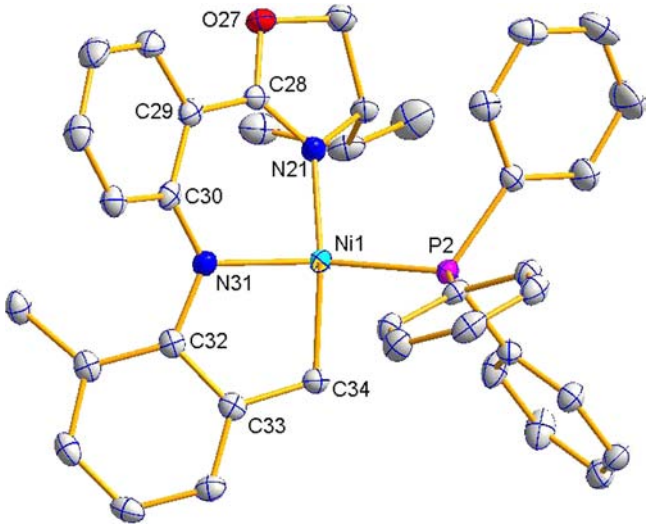

Figure 2. Molecular structure of compound **3a** with thermal ellipsoids drawn at the 50% probability level.

donors in pincer systems, the N_{amido}–Ni–P bond angles of ~153° are much smaller than the typical linear arrangement for the trans angles involving the central atom of the pincer ligand.[28] Presumably, this reflects a rather strong steric strain of the nickel coordination environment. Consistent with this, the two adjacent chelating rings deviate significantly from coplanarity, with dihedral angles of 22.7(1)° (**3a**), 23.9(2)° (**3b**), and 23.6(1)° (**3c**), respectively. The six member ring adopts an envelope-like conformation with the Ni atom in the flap position. The Ni atoms are displaced by 0.6571(2) (**3a**), 0.6650(6) (**3b**), and 0.6984(3) (**3c**) Å from the plane through other five atoms of the six member rings. The dihedral angles between the aniline phenyl ring and the central phenyl skeleton ring are in the range 46.9(1)° (**3a**), 48.6(2)° (**3b**), and 50.0(1)° (**3c**).

Comparison of structural features of complexes **3b** and **3c** suggests that the absolute configuration at the 4-oxazoline position has a profound influence on the overall configuration of the complexes. A side-by-side comparison of structures of **3b** and **3c**, roughly along the C–Ni–N_{imino}, is shown in Figure 3. The 2,6-disubstituted aniline phenyl moiety bends toward the same direction of the substituent at the oxazoline chiral center, while the backbone aromatic ring, as well as the PPh_3 group, points toward the opposite direction, to minimize the steric interactions.

Racemization and Structure of 3d. When ligand **2d**, with a phenyl substituent at the 4-oxazoline position, was employed, similar benzylic C–H activation occurred and CNN pincer complex was readily obtained. However, the chiral center at the 4-oxazoline position somehow racemized. The compound crystallized in a different crystal system (triclinic for **3d** vs orthorhombic for **3a–c** and **3e**) that contains a pair of enantiomers in the unit cell related by an inversion center.[22] The geometrical parameters are similar to those in **3a–c**, but the distortion appears to be less severe. The racemization of **3d** is further supported by the CD measurement, which showed no observable signals. In comparison, the CD spectrum of ligand **2d** showed distinctive features. Moreover, the single crystal X-ray structure of **2d** was determined, which is in accordance with the ligand chirality with the same absolute configuration (*R*) at the 4-oxazoline position as the starting (*R*)-2-phenylglycinol. Additionally, the free ligand itself takes on a planar configuration with the N–H proton located between amido and imino nitrogens, forming an intramolecular N–H···N hydrogen bond. The dimethyl phenyl unit resides nearly perpendicular to the above-mentioned plane. Comparison with the ligand parameters in the nickel complex further confirmed the distortion upon coordination (Figure 4). Particularly, the nearly coplanar oxazoline ring and the central phenyl ring in the free ligand are now twisted at 25.20(5)°, and the dihedral angle between the aniline phenyl ring and the central phenyl skeleton ring is 59.01(5)° in the complex.

Synthesis and Structure of 3e. Inspired by the formation of complexes **3a–d**, we were interested to see if C–H bonds other than the benzylic one can be activated and form pincer complexes within this type of ligands. Thus, ligand **2e**, in which a chiral alkyl moiety was introduced adjacent to the amine nitrogen, was examined. Following a similar procedure, a dark red crystal was obtained from reaction of *trans*-NiCl(Ph)-$(PPh_3)_2$ and in situ generated lithium salt of ligand **2e**. The ^1H NMR spectrum in benzene-d_6 showed the absence of the N–H signal of the free ligand. The benzylic proton, however, is still observed at 4.99 ppm as a quartet, shifted downfield compared with free ligand (4.55 ppm). These observations are consistent with a proposed structure with C_1 symmetry (Scheme 3).

X-ray crystal structure analysis confirmed the pincer coordination mode of the ligand, in which the cyclometalation takes place on the *ortho*-phenyl position of the amine arm to form a five-membered chelation ring (Figure 5). Selected bond lengths and bond angles are listed in Table 2. Unlike complexes **3a–d**, one Cl atom is coordinated to Ni atom instead of PPh_3. The nickel atom resides in a distorted square planar geometry constructed by N3, N14, C17, and Cl2 with the bond distances of N3–Ni1 = 1.942(4), N14–Ni1 = 1.887(4), C17–Ni = 1.887(5), and Ni–Cl2 = 2.210(2) Å. Clearly the Ni–C17 bond distance is much shorter than those in complexes **3a–d**. Presumably, this is because the PPh_3 group was replaced by a smaller Cl atom, which reduces steric crowdedness around the metal center. In addition, PPh_3 has a much stronger trans influence than chloride, further lengthening the Ni–C distance in **3a–d**. Absence of PPh_3 ligand makes the nickel coordination environment more planar, and the deviation of Ni from the coordination plane is only 0.0354(6) Å. $Li(OPPh_3)_4^+$ is found

Table 2. Selected Bond Distances (Å) and Bond Angles (deg) in Complexes 3a–e Determined by X-ray Crystallography

	3a	3b	3c	3d	3e
Ni–C	1.9320 (15)	1.934(4)	1.9303(18)	1.9308(15)	1.887(5)
Ni–N_{amido}	1.9197 (14)	1.914(4)	1.9177(16)	1.9081(11)	1.887(4)
Ni–N_{imino}	1.9199 (14)	1.926 (4)	1.9343(17)	1.9358(12)	1.942(4)
Ni–P/Cl	2.1335(4)	2.1327(12)	2.1333(5)	2.1631(4)	2.2100(15)
N_{imino}–Ni–C	162.77(7)	164.05(19)	162.74(8)	171.60(6)	176.1(2)
N_{amido}–Ni–P/Cl	152.69(4)	153.91(12)	152.84(5)	167.39(4)	174.92(12)

dx.doi.org/10.1021/ic3021904 | *Inorg. Chem.* 2013, 52, 1454–1465

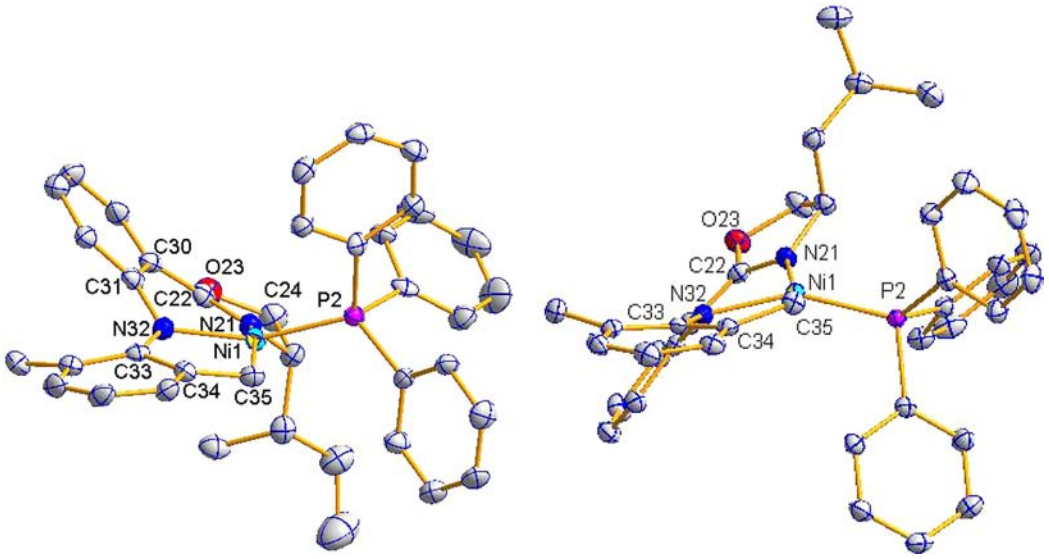

Figure 3. Side view of the structures **3b** (left) and **3c** (right).

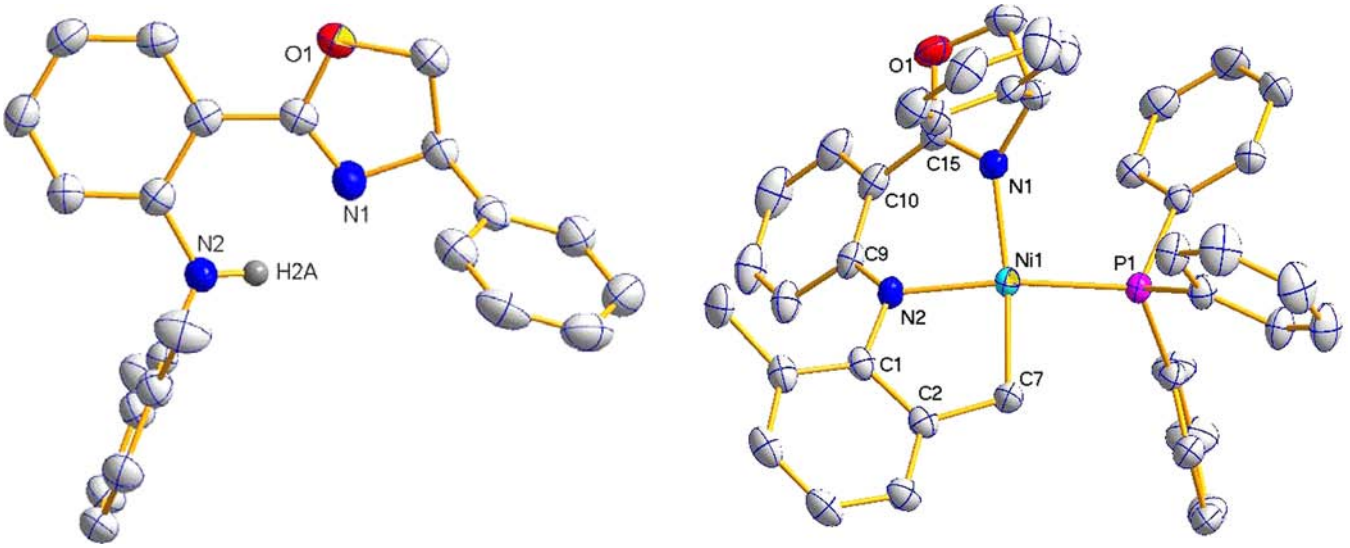

Figure 4. Molecular structure of ligand **2d** (left) and its nickel complex **3d** (right).

Scheme 3. Synthesis of Pincer Complexes 3e

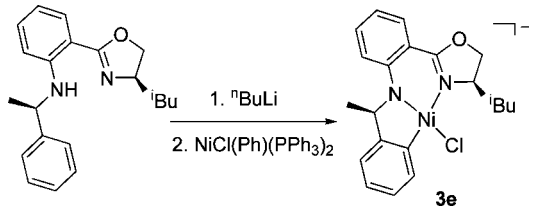

as the countercation in the crystal structure; presumably oxygen comes from adventitious air during the reaction process.

UV–vis and CD Spectroscopy of Ni Complexes 3a–3d. UV–vis and CD spectra of Ni complexes **3a–3d** are presented in Figure 6 and summarized in the Experimental Section. In general, all complexes exhibit four features in their UV–vis spectra. The first low intensity band ($\varepsilon \sim 200$ M^{-1} cm^{-1}) is located at ~650 nm, which follows by two intense bands at ~440 ($\varepsilon \sim 2500$ M^{-1} cm^{-1}) and ~320 ($\varepsilon \sim 9000$ M^{-1} cm^{-1}) nm bands with one low-intensity broad shoulder observed at ~500 nm. The CD spectra of the Ni complexes **3a–3d** are shown in Figure 6 and agree well with the UV–vis spectra. All (*R*)-isomers have a strong *negative* signal, which corresponds to the low-energy transition observed in UV–vis spectra at ~650 nm. This band follows the low-intensity negative signal at ~510 nm, which correlates with the position of shoulder observed in UV–vis spectra of corresponding complexes. Absorption band at ~440 nm has a positive amplitude for all (*R*)-isomers and fits well with a position of intense band observed in UV–vis spectra of the target nickel complexes. Finally, one low intensity (~380 nm) and one high-intensity negative CD signal dominate in the UV region of the CD spectra of complexes **3a–3d**. In agreement with the expectations, the CD spectrum of the (*S*)-isomer of complex **3c** is a mirror image of the CD spectrum of the (*R*)-isomer. As it has already been mentioned above, complex **3d** has no signals in CD spectrum, which confirms its racemization during a metal-insertion reaction.

DFT-PCM and TDDFT-PCM Calculations. A tentative interpretation of the UV–vis and CD spectra of nickel(II)

dx.doi.org/10.1021/ic3021904 | *Inorg. Chem.* 2013, 52, 1454–1465

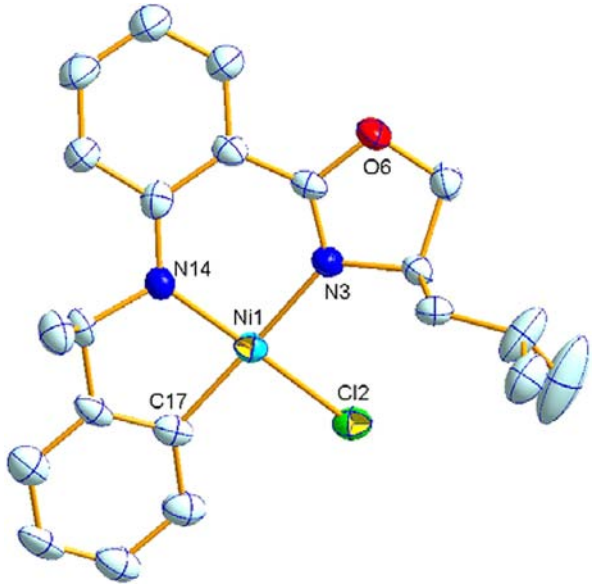

Figure 5. X-ray crystal structure of compound **3e.** Cationic counterion is omitted for clarity.

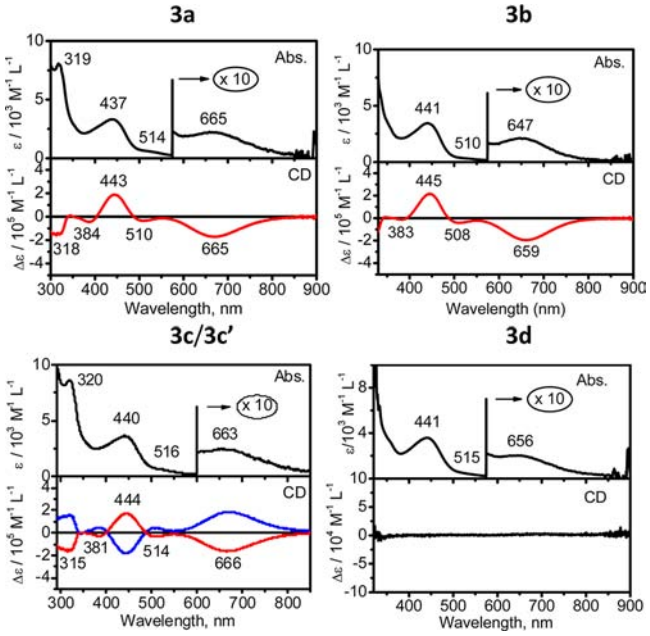

Figure 6. UV−vis and CD spectra of **3a**−**3d** in CH_2Cl_2.

complexes **3a**−**3d** is quite challenging. In particular, the following questions should be addressed: (i) taking into consideration the "soft base" character of new CNN pincer ligand, is the highest occupied molecular orbital (HOMO) predominantly nickel- or CNN π-centered MO? (ii) is the lowest unoccupied molecular orbital (LUMO) π^* MO centered on the pincer CNN ligand or the soft PPh_3 fragment? (iii) are the low-intensity band at∼665 nm and a shoulder at ∼510 nm classic nickel(II) d-d transitions? (iv) is the intensive band observed at ∼440 nm charge-transfer or $\pi-\pi^*$ in nature? Thus, the further insight into the electronic structure and UV−vis as well as CD spectroscopy of the target nickel complexes **3a**−**3d** was gained on the basis of DFT-PCM and TDDFT-PCM calculations which have been shown to provide accurate energetic and spectroscopic parameters for a large variety of transition-metal complexes[29] including nickel-containing compounds.[30] Since UV−vis and CD spectra of all investigated nickel complexes are very close to each other, we have only calculated electronic structure, UV−vis, and CD spectra of (*R*)- and (*S*)-isomers of complex **3c**. As shown in the Supporting Information, Table S1, the predicted geometries from DFT-PCM calculations are in good agreement with the X-ray experimental parameters. The DFT-PCM predicted MO energy diagram for **3c** is presented in Figure 7, while an analysis of the

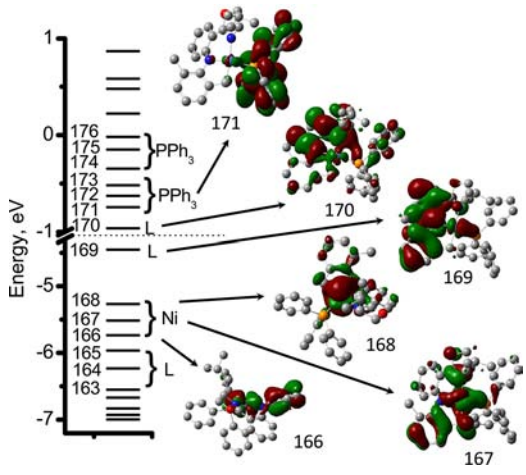

Figure 7. Molecular energy diagram and frontier orbitals of complex **3c** calculated using DFT-PCM approach and X3LYP exchange-correlation functional. HOMO−LUMO energy gap is indicated by the dotted line.

orbital compositions is provided in Figure 8 and Supporting Information, Table S2. In addition, the frontier orbitals of the complex **3c** are also pictured in Figure 7.

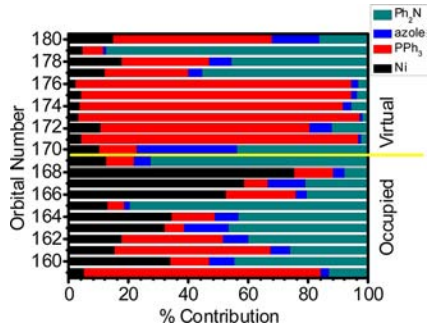

Figure 8. Molecular orbitals contribution analysis of complex **3c** calculated at DFT-PCM level using X3LYP exchange-correlation functional. Black bars are the contribution of Ni ion, red bars are the contribution of PPh_3 ligand, blue bars are the contribution of oxazoline part of the pincer ligand, bluegray bars are the contribution of PhNPh part of the pincer ligand.

The X3LYP/6-31G(d) DFT-PCM calculations predict that the HOMO in the complex **3c** is a predominantly π-orbital with an electron density delocalized over diphenylamide fragment of the ligand with the metal contribution of ∼10%. This orbital is energetically well-separated (∼0.8 eV) from the closely spaced predominantly nickel-centered HOMO-1 to HOMO-3 MOs. HOMO-1 is dominated by a nickel d_{z^2} AO contribution, while HOMO-2 and HOMO-3 have prominent nickel d_{xz} and d_{yz} characters, respectively. The other set of MOs, which is

dx.doi.org/10.1021/ic3021904 | *Inorg. Chem.* 2013, 52, 1454−1465

important for understanding of the UV−vis and CD spectra of **3c** (HOMO-4 to HOMO-9), is predominantly localized over PPh_3 and chiral pincer ligands (Figures 7 and 8 and Supporting Information, Table S2). For instance, HOMO-4 has distinct π-character and is localized over $C_6H_3CH_2$ fragment. Similarly, HOMO-5 and HOMO-6 are π-orbitals delocalized over the pincer ligand, while HOMO-7 and HOMO-8 have distinct PPh_3 localization. Except LUMO+2, which has ∼10% of nickel $d_{x^2-y^2}$ character, LUMO to LUMO+10 MOs are dominated either by PPh_3 (LUMO+1 to LUMO+6) or pincer ligand (LUMO, LUMO+7 to LUMO+9) contributions and could be characterized as π^* MOs.

The further interpretation of the UV−vis and CD spectra of complex **3c** was solidified on the basis of TDDFT-PCM calculations (Figure 9 and Supporting Information). TDDFT-PCM predicted vertical excitation energies, oscillator strengths, and rotary strengths of **3c** calculated with and without solvent equilibration are virtually identical. UV−vis and CD spectra in the 400−900 nm range could be described using the first six low-energy excitations. The first low-intensity band experimentally observed as a weak band at ∼665 nm in UV−vis spectrum and as a strong positive signal in the CD spectrum of **3c** is associated with the first transition predicted by the TDDFT-PCM method. This excited state (Supporting Information) consists of 10 significant single-electron contributions, has ∼74% of intra- and interligand $\pi-\pi^*$ character, and ∼26% of metal-to-ligand charge-transfer (MLCT) character, and dominated by HOMO → LUMO (∼47%) and HOMO → LUMO+2 (∼14%) transitions. The first transition has intra(pincer)-ligand character, while the second one can be described as the charge-transfer transition from the pincer ligand to PPh_3 fragment. In agreement with experimental data, the oscillator strength of this transition is small, while rotary strength is positive and large. The second and third excited states are responsible for the broad, low intensity shoulder observed in UV−vis spectrum of **3c** between 500 and 600 nm and weak positive CD signal observed in the same region.

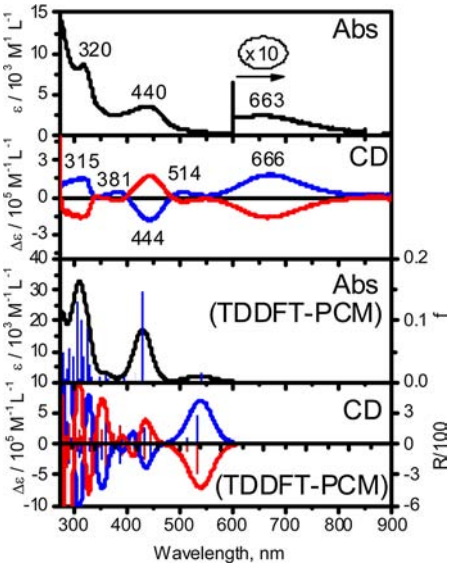

Figure 9. Experimental UV−vis and CD data (top) and TDDFT-PCM predicted UV−vis and CD spectra (bottom) of complex **3c**. Blue lines represent the (*S*)-isomer and red lines represent the (*R*)-isomer of the chiral complex.

These transitions have pure MLCT character and are dominated by HOMO-1 (Ni d_{z^2}) → LUMO (∼40%, pincer π^* MO), LUMO+2 (∼25%, PPh_3 π^* MO) for excited state 2 or HOMO-2 (Ni d_{xz}) → LUMO, LUMO+2 (∼25%, pincer π^* MO), LUMO+2 (∼20%, PPh_3 π^* MO) for excited state 3 transitions. In addition, ∼22% of excited state 3 could be described as HOMO-3 (Ni d_{yz}) →LUMO, LUMO+1, LUMO +7, and LUMO+8 single-electron excitations. Again, in agreement with experimental data, TDDFT-PCM predicted rotary strengths of the excited states 2 and 3 are positive and significantly smaller compared to that in the first excited state. According to TDDFT-PCM calculations, excited state 4 is the main contributor to the 440 nm band observed in UV−vis spectrum of **3c**. This excited state consists of five major single-electron contributions, has ∼90% of $\pi-\pi^*$ character, and dominated by HOMO → LUMO (∼64%) and HOMO → LUMO+2 (∼26%) transitions. In agreement with experimental CD spectrum, TDDFT-PCM calculations predict strong negative signal associated with this excited state. Excited state 5 could be associated with the higher-energy shoulder of the 440 nm band, a positive signal in the CD spectrum observed at ∼375 nm. This excited state has 17 single-electron contributions, has ∼83% of $\pi-\pi^*$ and ∼17% of MLCT character, and has no dominant contribution (the largest single-electron contribution is ∼11% for HOMO → LUMO+2 transition). Again, TDDFT-PCM calculations predict positive amplitude for the CD signal associated with this excited state. Finally, the shoulder at ∼350 nm observed in the UV−vis spectrum of **3c** and a weak negative signal observed in its CD spectrum in this region can be assigned to the excited state 6. This excited state has pure $\pi-\pi^*$ character and could be described as almost pure HOMO → LUMO+1 (PPh3, π^* MO) single electron transition (∼96%). TDDFT-PCM calculations predict that the higher energy regions of UV−vis and CD spectra of **3c** consist of numerous overlapping excited states and thus it is impossible to provide a clear assignment for intense 320 nm and higher energy bands.

Overall, TDDFT-PCM calculations are in a good agreement with the experimental UV−vis and CD data and allow to assign the observed spectra in the 400−900 nm region to four excited states with predominantly $\pi-\pi^*$ character and two excited states with predominantly MLCT character.

DISCUSSIONS

A few anilido imine complexes of nickel have been reported as analogues of conventional β-diketimine or α-diimine based complexes, mostly for applications in catalystic olefin polymerization.[31] Usually they are obtained as mono- or dinuclear Ni(II) species by reaction of free or deprotonated ligands with a nickel precursor such as $Ni(OAc)_2$, $NiCl_2$, $NiBr_2$, $NiCl_2(THF)_{1.5}$, $NiCl_2(py)_4$, and $Ni(acac)_2$, with or without the presence of a base. When *trans*-$NiCl(Ph)(PPh_3)_2$ was employed as the precursor, formation of a three coordinate Ni(I) complex (**NN**)$Ni^I(PPh_3)$ was observed.[27a,32] Analogous results were obtained for the conventional β-diketiminato ligand, leading to reduction of Ni(II) and formation of three coordinate Ni(I) complexes.[33] However, when less bulky ketiminato and salicylaldiminato ligands were allowed to react with *trans*-$NiCl(Ph)(PPh_3)_2$, square planar Ni(II) complexes from simple metathesis were obtained as the main products.[33,34] It should be emphasized that in none of these reactions C−H activation of ligands has been observed. Therefore, it is surprising to note that in the present system,

dx.doi.org/10.1021/ic3021904 | *Inorg. Chem.* 2013, 52, 1454−1465

one of the benzylic or aryl C−H bonds on the aniline side arm was cyclometalated, and the ligand functioned as a tridentate, dianionic chelate and led to the formation of unsymmetric CNN pincer type complexes.

A large number of pincer complexes with a C backbone or arm have been prepared; the vast majority of them are introduced through direct metalation, transmetalation, or cyclometalation of C(sp^2)-H bonds.[8] In comparison, examples with C(sp^3)-H bonds, either benzylic or aliphatic, are relatively less common,[12,35] although the coordination-assisted C(sp^3)-H bond activation by palladium is well-documented.[36] It also appears that the metalation occurs only when the metal center is easily accessible to the CH bond so that substitution at the sp^3 carbon is feasible.[37] Thus, the results here are even more striking, considering the typical orientation that the *ortho*-dimethyphenyl group adopts and the strong distortion the ligand would have to go through to form the observed complexes. We have described the distorted coordination environment around the Ni center. The sensitivity of these complexes toward air may also be a reflection of the strain in the system.

Another puzzling yet important aspect is the observation of racemization of chiral oxazolines in compound **3d**, apparently during the complex formation. Oxazoline and its derivatives have been employed extensively in transition metal asymmetric catalysis,[38] but racemization of chiral oxazolines upon metal coordination or during catalysis is rarely reported. Gabbai and co-workers noted that a chiral oxazoline palladium complex, (*S,S*)-di-μ-(acetate)-bis[2-[2-(4-carbomethoxy) oxazolinyl]-phenyl-C,N]-dipalladium(II), underwent racemization reaction when serving as a catalyst for the hydrolysis of organo-phosphorus.[39] However, the mechanism of racemization is not well-understood. One possibility is that deprotonation of hydrogen at 4-oxazoline may occur because of the enhanced acidity when a phenyl (as in **3d**) or carbomethoxy (as in the dipalladium complex) group is attached. Isomerization to 3-oxazoline or nonselective recombination of proton and carbanion resulted in racemization (Scheme 4). It is unclear

Scheme 4. Possible Pathways for Racemization of 3d

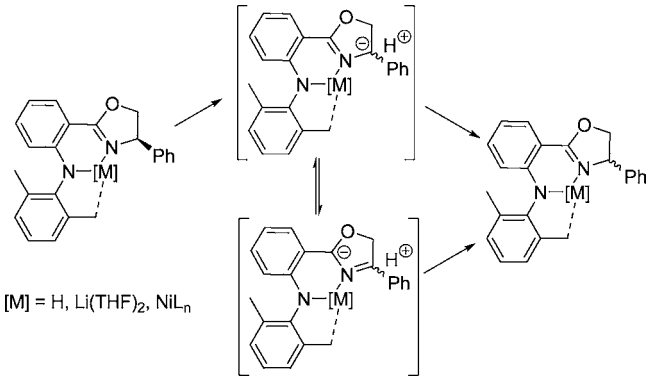

what could serve as a base to deprotonate the 4-H. Fortunately, no racemization is observed when aliphatic substituents are present at the 4-oxazoline position, as seen in **3a−c** in our study.

It has been suggested that the steric bulk of the chelating NN ligands in combination of the bulky PPh_3 played a key role in the reduction of Ni(II) and the formation of three-coordinated Ni(I).[27a] We suspect that unexpected formation of CNN pincer complexes via C−H activation may have a similar steric origin. Presumably, the ligand is first coordinated to nickel(II) in an N,N-bidentate fashion, with PPh_3 in the less congested side and phenyl group adjacent to the aniline moiety. Because of the proper steric interaction with the environment, particularly the chiral oxazoline quadrant, the dimethylphenyl group was forced out of its normal perpendicular position, with one methyl leaning close toward the Ni center. This may lead to an agostic interaction or a σ-complex that eventually resulted in the elimination of benzene and the formation of the carbon nickel bond, possibly through a conventional concerted σ-bond metathesis or a σ-complex assisted metathesis pathway (Scheme 5). Such mechanisms are common for electrophilic

Scheme 5. Possible Pathway for Complexes 3a−d

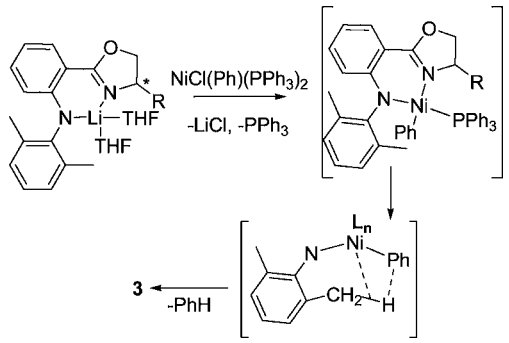

early transition metal systems,[40] but it can occur with late transition metals as well.[41] The observation of the nickel product in the same oxidation state and the absence of biphenyl from phenyl coupling in the products are in agreement with this mechanism. An oxidative addition pathway involving a high valent nickel, formally Ni^{IV}, seems less likely, but could not be ruled out.[42] Further studies are required to elucidate the reaction mechanism and to utilize this C−H activation chemistry.

One of our initial goals is to prepare nickel(II) complexes incorporating chiral, monoanionic β-diketimine type ligands. Therefore, we explored a number of commonly used nickel precursors listed above in the synthesis. Though signs of reactions were noted in several occasions, only the procedure with *trans*-NiCl(Ph)(PPh_3)$_2$ afforded the isolable and identifiable nickel complexes, leading to the formation of pincer complexes via unexpected C−H activation. However, the yields are generally low; and the highest so far obtained is ~35% with **3a**, despite numerous attempts to improve the reactions.

Efforts were also made to isolate and characterize other Ni-containing products formed in the reaction. The paramagnetic species were often observed in the crude reaction mixture, as indicated by the appearance of ^{1}H NMR signals in the +50 and −50 ppm range. Another type of byproduct features two nickel centers without incorporation of the anilido imine ligands. One of them was isolated as dark-green crystals and characterized by X-ray diffraction crystallography, which revealed a dinuclear structure of (PPh_3)$_2$Ni(μ-PPh_2)$_2$Ni(PPh_3), **4**.[22] These observations may explain, at least in part, the low yields generally obtained, and they also indicate the complexity of the process.

■ CONCLUSIONS

In summary, we have synthesized and characterized a series of chiral and unsymmetrical CNN pincer nickel complexes with

dx.doi.org/10.1021/ic3021904 | *Inorg. Chem.* 2013, 52, 1454−1465

C_1 symmetric ligands via a coordination assisted cyclometalation process. Both C(sp^3)-H and C(sp^2)-H bonds may be activated, showing the diversity it may bring. The absolute configuration of chiral groups exerts considerable influence on the overall structural arrangement. The fact that both benzylic and aryl C−H bonds are activated with similar ease suggests that the geometries of the intermediates favor activation, regardless of the energetics of the process. These findings open a new possibility for a pincer ligand design based on the anilido imine framework and appear promising for further investigations. Current efforts aim to establish the general applicability of the synthetic approach, further probe the origin of the observed activity by varying substituent groups on both arms, and explore if the activity can be harnessed for practical C−H activations. In addition, these nickel complexes are chiral with easily tunable substituents, and their potential applications in asymmetric catalysis will be investigated.

EXPERIMENTAL SECTION

General Procedures. All air- or moisture-sensitive reactions were carried out under a dry nitrogen atmosphere, employing standard Schlenk line and drybox techniques. Tetrahydrofuran, toluene, and diethyl ether were dried over potassium hydroxide and distilled over Na/benzophenone prior to use. Dimethylformamide (DMF) was distilled over CaH_2. Deuterated solvents were purchased from Cambridge Isotope Laboratory, dried over sodium or calcium hydride, degassed, and distilled by vacuum transfer. *trans*-NiCl(Ph)(PPh_3)$_2$ was prepared according to a literature procedure.[43]

All ^{1}H and ^{13}C NMR spectra were recorded on a Bruker AVANCE-500 NMR spectrometer and referenced to TMS or the residue peaks in $CDCl_3$ or C_6D_6. ^{31}P NMR was referenced to P(OEt)$_3$ at 137 ppm. The elemental analysis was performed by Midwest Microlab, Indianapolis, IN. UV−vis data were obtained on Jasco-720 or Cary 17 spectrophotometers. Circular Dichroism (CD) data were recorded using OLIS DCM 17 CD spectropolarimeter. GC-MS analyses were performed on an HP 5890 GC/HP 5971/B MSD system with electron impact ionization (70 eV).

Ligand 2e by Cu-Catalyzed Amination.[21] An oven-dried Schlenk flask was charged with a magnetic stir bar, CuI (10 mg, 0.05 mmol, 5 mol %) and K_3PO_4 (2 mmol, 425 mg), then evacuated and backfilled with nitrogen three times. Under a counter-flow of nitrogen, *R*-(+)-α-methylbenzylamine (181 mg, 1.5 mol), oxazoline derivative (302 mg, 1 mmol), and DMF (0.5 mL) were added by syringe. Finally, 2-isobutyrylcyclohexanone (34 mg, 0.2 mmol, 20 mol %) was added via syringe, the flask was sealed, and the mixture was heated at the 110 °C for 24 h. Upon completion of the reaction, the mixture was allowed to cool to room temperature, diluted with ethyl acetate, and passed through a fritted glass filter to remove the inorganic salts. The solvent was removed with the aid of rotary evaporator. The residue was purified by column chromatography on silica gel, and the product was dried under vacuum for at least 1 h. Colorless crystals of the product could be obtained in ethyl acetate by slow evaporation. The typical yield was ∼40%. The identity of **2e** was compared with literature[20a] and confirmed by ^{1}H NMR and GC-MS.

Lithium Salt L^{2d}Li(THF)$_2$. Ligand **2d** (1 mmol) was dissolved in 10 mL of THF and cooled to −78 °C. To it was added an *n*-butyl lithium solution in hexane (0.625 mL, 1.6 M) at low temperature. The solution changed from colorless to dark-green and then orange. It was allowed to stir for 2 h at −78 °C and then warm to room temperature with stirring. THF was then removed under vacuum, and the yellow residue was washed with hexane. Light yellow needle-like crystals could be obtained by diffusion of hexane into a THF solution of the lithium salt. The yield is 0.39 g (80%). ^{1}H NMR (500 MHz, C_6D_6): δ 8.40 (d, 1 H, J = 8.41 Hz), 7.21 (m, 3 H), 7.13 (m, 1 H), 6.99 (m, 5 H), 6.58 (d, 1 H, J = 6.55 Hz), 6.48 (t, 1 H, J = 6.47 Hz), 4.78 (t, 1 H, J = 4.78 Hz), 4.16 (t, 1 H, J = 4.15 Hz), 3.72 (t, 1 H, J = 3.70 Hz), 3.11 (m, 8 H, THF), 2.36 (s, 3 H), 2.31 (s, 3 H), 1.13 (m, 8 H, THF) ppm. ^{13}C NMR (126 MHz, C_6D_6): δ 170.32, 158.76, 153.66, 144.70, 133.88, 133.28, 133.21, 133.17, 129.23, 128.87, 127.27, 121.59, 115.68, 109.10, 105.69, 73.27, 70.09, 68.13 (THF), 25.68 (THF), 19.31, 19.23.

Synthesis of 3a. The following procedure is typical: **2a** (30.8 mg, 0.1 mmol) was dissolved in 5 mL of THF which was cooled to −78 °C. At this temperature 50 μL of BuLi (0.1 mmol) was added, and the resulting yellow solution was stirred at low temperature for 1 h and then was allowed to warm to room temperature. All volatiles were removed under vacuum. The yellow residue was dissolved in 5 mL of toluene, and then mixed with the orange solution of NiCl(Ph)(PPh_3)$_2$ (0.1 mmol) in 5 mL of toluene. The red to dark-red solution was stirred overnight at ambient temperature. After filtration and removal of solvent, the residue was dissolved in a small amount of toluene and layered up with hexanes. After a few days, the red crystals formed and were collected. The yield is 22 mg (35%).^{1}H NMR (500 MHz, C_6D_6): δ 7.92 (d, J = 7.9 Hz, 1H), 7.79−7.65 (m, 6H, *o*-PPh$_3$), 7.12−7.06 (m, 1H), 7.06−6.99 (m, 3H), 6.99−6.89 (m, 9H, *m,p*-PPh$_3$), 6.76 (t, J = 7.3 Hz, 1H), 6.52 (t, J = 7.2 Hz, 1H), 3.57 (dd, J = 8.6, 2.2 Hz, 1H, NCH(R)CH_2O), 3.31 (t, J = 8.6 Hz, 1H, NCH(R)CH_2O), 2.76 (dd, J = 13.5, 5.0 Hz, 1H, NiCH_2), 2.54−2.42 (m, 1H, NCH(R)CH$_2$O), 2.19 (s, 3H, ArCH_3), 2.04−1.96 (m, 1H, CHMe$_2$), 1.38 (dd, J = 14.3, 14.3 Hz, 1H, NiCH_2), 0.74 (d, J = 6.7 Hz, 3H, CHMe_2), 0.28 (d, J = 6.9 Hz, 3H, CHMe_2). ^{13}C NMR (126 MHz, C_6D_6): δ 163.57, 156.54, 155.37, 145.66, 134.66, 133.79, 133.48, 133.15, 130.34, 129.53−128.08, 126.92, 124.68, 120.53, 119.87, 112.90, 111.24, 69.81 (NCH(R)-CH$_2$O), 67.73 (NCH(R)CH_2O), 33.44 (CHMe$_2$), 26.43 (d, $^2J_{C-P}$= 25.3 Hz, NiCH_2), 21.05 (ArCH_3), 18.56 (CHMe_2), 15.40 (CHMe_2). ^{31}P NMR (202 MHz, C_6D_6): δ 32.04. UV−vis (DCM, ε M^{-1} cm^{-1}): 319 (8010), 437 (3310), 514sh (622), 665 (220).

Synthesis of 3b. The procedure is the same as **3a** while ligand **2b** (32.2 mg, 0.1 mmol) was used. The yield is 15.2 mg (24%). Elemental analysis: Calc. $C_{39}H_{39}N_2NiOP$, C, 73.03; H, 6.13; N, 4.37. Found: C, 72.74; H, 5.99; N, 4.26. ^{1}H NMR (500 MHz, C_6D_6): δ 7.93 (dd, J = 7.9, 1.6 Hz, 1H), 7.75−7.66 (m, 6H, *o*-PPh$_3$), 7.16 (s, 2H), 7.12−7.01 (m, 3H), 6.94 (m, 9H, *m,p*-PPh$_3$), 6.77 (t, J = 7.3 Hz, 1H), 6.53 (ddd, J = 7.9, 6.7, 1.2 Hz, 1H), 3.58 (dd, J = 8.7, 2.9 Hz, 1H, NCH(R)CH_2O), 3.27 (t, J = 8.7 Hz, 1H, NCH(R)CH_2O), 2.66 (dd, J = 13.8, 5.5 Hz, 1H, NiCH_2), 2.60 (dt, J = 8.6, 2.9 Hz, 1H, NCH(R)CH$_2$O), 2.20 (s, 3H, ArCH_3), 1.96−1.90 (m, 1H, CHCH$_3$(Et)), 1.45 (dd, J = 14.2, 14.2 Hz, 1H, NiCH_2), 0.70 (d, J = 6.8 Hz, 1H, CHCH_3(Et)), 0.49 (t, J = 6.0 Hz, 3H, CHCH$_3$(CH$_2$CH_3)), 0.47−0.40 (m, 2H, CHCH$_3$(CH_2CH$_3$)). ^{13}C NMR (126 MHz, C_6D_6): δ 163.62, 156.48, 155.31, 145.55, 145.50, 134.69, 134.61, 133.58, 133.26, 133.11, 130.37, 130.23, 126.91, 124.83, 120.47, 119.86, 112.88, 111.10, 69.23 (NCH(R)CH$_2$O), 67.63 (NCH(R)CH_2O), 40.47 (CHCH$_3$(Et)), 26.38 (d, $^2J_{C-P}$= 25.3 Hz, NiCH_2), 26.29 (CHCH_3(CH_2CH$_3$)), 21.08 (ArCH_3), 12.41 (CHCH_3(CH_2CH_3)), 11.85 (CHCH_3(CH_2CH$_3$)). ^{31}P NMR (202 MHz, C_6D_6): δ 33.02. UV−vis (DCM, ε M^{-1} cm^{-1}): 441 (3490), 510sh (390), 647 (210).

Synthesis of 3c. The procedure is the same as **3a**. **2c** (32.2 mg, 0.1 mmol) was used. Yield: ∼15%. ^{1}H NMR (500 MHz, C_6D_6): δ 7.99 (d, J = 8.5 Hz, 1H), 7.74 (dd, J = 9.4, 7.7 Hz, 6H, *o*-PPh$_3$), 7.12−7.07 (m, 3H), 6.99−6.89 (m, 10H, *m,p*-PPh$_3$+ArH), 6.79 (t, J = 7.3 Hz, 1H), 6.56 (ddd, J = 7.9, 5.5, 2.3 Hz, 1H), 3.50 (dd, J = 8.2, 2.7 Hz, 1H, NCH(R)CH_2O), 3.23 (t, J = 8.1 Hz, 1H, NCH(R)CH_2O), 2.52−2.44 (m, 2H, NCH(R)CH$_2$O + NiCH_2), 2.21 (s, 3H, ArCH_3), 1.89−1.80 (m, 1H, CH_2CHMe$_2$), 1.64 (dd, J = 13.8, 13.8 Hz, 1H, NiCH_2), 1.18 (ddd, J = 13.8, 11.1, 4.9 Hz, 1H, CH_2CHMe$_2$), 1.03−0.94 (m, 1H, CH$_2$CHMe$_2$), 0.61 (d, J = 6.6 Hz, 3H, CH$_2$CHMe_2), 0.28 (d, J = 6.6 Hz, 3H, CH$_2$CHMe_2). ^{13}C NMR (126 MHz, C_6D_6): δ 163.96, 156.19, 155.27, 145.13, 134.92, 134.83, 133.37, 133.09, 132.99, 130.40, 130.06, 128.89, 128.79, 127.01, 124.94, 120.35, 120.01, 112.91, 110.95, 71.35 (NCH(R)CH$_2$O), 63.89 (NCH(R)CH$_2$O), 45.83 (CH$_2$CHMe$_2$), 26.61 (d, $^2J_{C-P}$ = 26.5 Hz, NiCH_2), 25.69 (CH$_2$CHMe$_2$), 24.08 (ArCH_3), 22.02 (CH$_2$CHMe_2), 21.38 (CH$_2$CHMe_2). ^{31}P NMR (202 MHz, C_6D_6): δ 34.20. UV−vis (DCM, ε M^{-1} cm^{-1}): 320 (8620), 440 (3620), 516sh (673), 663 (240). The complex **3c′** was prepared analogously, starting from ligand **2c′** with a (*S*)-^{i}Bu substituent at the 4-oxazoline position. The ^{1}H NMR data are virtually identical with **3c**.

Synthesis of 3d. The procedure is the same as **3a**. **2d** (34.2 mg, 0.1 mmol) was used. Yield: ∼20%. ^{1}H NMR (500 MHz, C_6D_6): δ 7.94

dx.doi.org/10.1021/ic3021904 | Inorg. Chem. 2013, 52, 1454−1465

(d, J = 8.5 Hz, 1H), 7.53 (m, 6H, o-PPh_3), 7.20−7.12 (m, 4H), 7.01−6.96 (m, 5H), 6.95 (m, 3H), 6.86 (td, J = 7.9, 5.0 Hz, 6H), 6.76 (t, J = 7.5 Hz, 1H), 6.55 (m, 1H), 3.58 (m, 1H, NCH(R)CH_2O), 3.50 (m, 2H, NCH(R)CH_2O), 2.48 (dd, J = 13.8, 5.5 Hz, 1H, NiCH_2), 2.29 (s, 3H, ArCH_3), 1.56 (m, 1H, NiCH_2). ^{13}C NMR (126 MHz, C_6D_6): δ 165.71, 156.11, 155.66, 145.13, 145.07, 143.01, 134.88, 134.79, 133.33, 133.28, 133.02, 130.29, 129.32, 126.97, 126.80, 124.90, 124.88, 120.47, 120.22, 120.21, 113.05, 110.55, 74.99 (NCH(R)CH_2O), 68.50 (NCH(R)CH_2O), 26.52 (d, $^2J_{C-P}$ = 25.2 Hz, NiCH_2), 21.43 (ArCH_3).^{31}P NMR (202 MHz, C_6D_6): δ 34.27. UV−vis (DCM, ε M^{-1} cm^{-1}): 441 (3590), 515sh (550), 656 (200).

Synthesis of 3e. The procedure is the same as **3a**. **2e** (0.1 mmol) was used. Yield: ∼10%. ^{1}H NMR (500 MHz, C_6D_6) δ 8.16 (t, J = 8.4 Hz, 2H), 7.82−7.56 (m, 24H), 7.20−6.96 (m, 40H), 6.48 (t, J = 7.2 Hz, 1H), 6.44 (t, J = 6.7 Hz, 1H), 4.99 (q, J = 5.8 Hz, 1H, NCH(Ar)CH_3), 4.85 (t, 1H, NCH(R)CH_2O), 3.73 (dd, J = 7.5, 2.5 Hz, 1H, NCH(R)CH_2O), 3.60 (t, J = 8.0 Hz, 1H, NCH(R)CH_2O), 2.38 (t, J = 10.6 Hz, 1H, CH_2CHMe$_2$), 1.63 (d, J = 6.1 Hz, 3H, NCH(Ar)CH_3), 1.45−1.39 (m, 1H, CH_2CHMe$_2$), 1.00 (m, 1H, CH_2CHMe$_2$), 0.97 (d, J = 6.4 Hz, 3H, CH_2CHMe_2), 0.65 (d, J = 6.5 Hz, 3H, CH_2CHMe_2). ^{31}P NMR (202 MHz, C_6D_6): δ 25.35. ^{13}C NMR was not obtained because of its low solubility.

X-ray Crystallography. Single crystal X-ray diffraction of compounds **2d**, **3d**, and **4** were collected on a Bruker Apex diffractometer equipped with an Oxford Cryosystems 700 Series Cryostream cooler, and that of compounds **3a−c** and **3e** were collected on a Rigaku RAPID II diffractometer equipped with XStream Cryosystem. Mo K_α radiation (λ = 0.71073 Å) was used on both instruments. X-ray crystal data, data collection parameters, and refinement parameters are summarized in Table 1 and more crystallographic details can be found in the Supporting Information.

DFT-PCM and TDDFT-PCM Calculations. The initial geometry of complex **3c** was taken from the X-ray data and optimized at the DFT level, using a hybrid X3LYP exchange-correlation functional. We choose this exchange-correlation functional after 12 exchange-correlation functional were compared for CD intensities calculations on chiral model nickel(II) complexes (full comparison on all tested exchange-correlation functional will be published elsewhere). Equilibrium geometries were confirmed by frequency calculations and specifically by the absence of the imaginary frequencies. Solvation effects were modeled using the polarized continuum model (PCM) approach.[44] DCM was used as the solvent in all calculations to match with experimental data. All single-point DFT-PCM and TDDFT-PCM calculations were conducted using a X3LYP functional.[45] The first 70 states were considered in all PCM-TDDFT calculations to cover UV and visible range of the spectrum. In all cases, 6-31G(d) basis set was used for all atoms.[46] All calculations were performed using Gaussian03 or 09 software. Molecular orbital analysis was conducted using the QMForge program.[47]

■ ASSOCIATED CONTENT

Supporting Information

Selected NMR, UV−vis, and CD spectra of **3a−d**, crystal packing of **3d**, molecular structure of **4**, and computational details in pdf, and crystal data for compound **2d**, **3a−e**, and **4** in cif. This material is available free of charge via the Internet at http://pubs.acs.org.

■ AUTHOR INFORMATION

Corresponding Author

*Tel: +1-701-777-2241 (G.D.), +1-218-726-6729 (V.N.N.). Fax: +1-701-777-2331 (G.D.). E-mail: gdu@chem.und.edu (G.D.), vnemykin@d.umn.edu (V.N.N.).

Present Address

[§]School of Chemistry and Chemical Engineering, University of Jinan, Jinan 250022, P.R. China.

Notes

The authors declare no competing financial interest.

■ ACKNOWLEDGMENTS

Financial support from ND EPSCoR through NSF Grant EPS-0814442 and the University of North Dakota is greatly appreciated. We are grateful to Dr. L. Stahl and Dr. Q. Chu for help with X-ray crystallography, Dr. K. Thomasson for a CD measurement, and Dr. P. Binda for initial investigations. Generous support from the NSF MRI CHE-0922366 (X-ray diffractometer), Minnesota Supercomputing Institute to V.N., and University of Minnesota UROP Grant to J.R.S. is greatly appreciated.

■ REFERENCES

(1) (a) van Koten. *Top. Organomet. Chem.* **2013**, *40*, 1−20 , and references therein. (b) Schneider, S.; Meiners, J.; Askevold, B. *Eur. J. Inorg. Chem.* **2012**, 412−429. (c) Nishiyama, H.; Ito, J.-I. *Chem. Commun.* **2010**, *46*, 203−212. (d) Pugh, D.; Danopoulos, A. A. *Coord. Chem. Rev.* **2007**, *251*, 610−641. (e) Dupont, J.; Consorti, C. S.; Spencer, J. *Chem. Rev.* **2005**, *105*, 2527−2572. (f) Peris, E.; Crabtree, R. H. *Coord. Chem. Rev.* **2004**, *248*, 2239−2246. (g) Albrecht, M.; van Koten, G. *Angew. Chem., Int. Ed.* **2001**, *40*, 3750−3781.

(2) (a) Bonnet, S.; Li, J.; Siegler, M. A.; von Chrzanowski, L. S.; Spek, A. L.; van Koten, G.; Klein Gebbink, R. J. M. K. *Chem.—Eur. J.* **2009**, *15*, 3340−3343. (b) Benito-Garagorri, D.; Kirchner, K. *Acc. Chem. Res.* **2008**, *41*, 201−213.

(3) Niu, J.-L.; Hao, X.-Q.; Gong, J. −F.; Song, M.-P. *Dalton Trans.* **2011**, *40*, 5135−5150.

(4) Moreno, I.; SanMartin, R.; Ines, B.; Herrero, M. T.; Dominguez, E. *Curr. Org. Chem.* **2009**, *13*, 878−895.

(5) (a) Balaraman, E.; Fogler, E.; Milstein, D. *Chem. Commun.* **2012**, *48*, 1111−1113. (b) Bossi, G.; Putignano, E.; Rigo, P.; Baratta, W. *Dalton Trans.* **2011**, 8986−8995. (c) Sun, Y.; Koehler, C.; Tan, R.; Annibale, V. T.; Song, D. *Chem. Commun.* **2011**, *47*, 8349−8351. (d) Fogler, E.; Balaraman, E.; Ben-David, Y.; Leitus, G.; Shimon, L. J. W.; Milstein, D. *Organometallics* **2011**, *30*, 3826−3833. (e) Kozlov, V. A.; Aleksanyan, D. V.; Nelyubina, Y. V.; Lyssenko, K. A.; Vasil'ev, A. A.; Petrovskii, P. V.; Odinets, I. L. *Organometallics* **2010**, *29*, 2054−2062. (f) Hao, X.-Q.; Wang, Y.-N.; Liu, J.-R.; Wang, K.-L.; Gong, J.-F.; Song, M.-P. *J. Organomet. Chem.* **2010**, *695*, 82−89. (g) Jones, G. D.; Martin, J. L.; McFarland, C.; Allen, O. R.; Hall, R. E.; Haley, A. D.; Brandon, J. R.; Konovalova, T.; Desrochers, P. J.; Pulay, P.; Vicic, D. A. *J. Am. Chem. Soc.* **2006**, *128*, 13175−13183. (h) Poverenov, E.; Gandelman, M.; Shimon, L. J. W.; Rozenberg, H.; Ben-David, Y.; Milstein, D. *Chem.—Eur. J.* **2004**, *10*, 4673−4684.

(6) (a) Gu, S.; Chen, W. *Organometallics* **2009**, *28*, 909−914. (b) Zhang, C.; Wang, Z.-X. *Organometallics* **2009**, *28*, 6507−6514. (c) Broring, M.; Kleeberg, C.; Kohler, S. *Inorg. Chem.* **2008**, *47*, 6404−6412.

(7) (a) Baratta, W.; Bosco, M.; Chelucci, G.; Del Zotto, A.; Siega, K.; Toniutti, M.; Zangrando, E.; Rigo, P. *Organometallics* **2006**, *25*, 4611−4620. (b) Baratta, W.; Ballico, M.; Del Zotto, A.; Herdtweck, E.; Magnolia, S.; Peloso, R.; Siega, K.; Toniutti, M.; Zangrando, E.; Rigo, P. *Organometallics* **2009**, *28*, 4421−4430.

(8) Selander, N.; Szabo, K. J. *Chem. Rev.* **2011**, *111*, 2048−2076.

(9) (a) Feng, J.-J.; Chen, X.-F.; Shi, M.; Duan, W.-L. *J. Am. Chem. Soc.* **2010**, *132*, 5562−5563. (b) Li, J.; Lutz, M.; Spek, A. L.; van Klink, G. P. M.; van Koten, G.; Gebbink, R. J. M. K. *Organometallics* **2010**, *29*, 1379−1387. (c) Iglesias-Sigueenza, J.; Ros, A.; Diez, E.; Magriz, A.; Vazquez, A.; Alvarez, E.; Fernandez, R.; Lassaletta, J. M. *Dalton Trans.* **2009**, 8485−8488. (d) Gosiewska, S.; Herreras, S. M.; Lutz, M.; Spek, A. L.; Havenith, R. W. A.; van Klink, G. P. M.; van Koten, G.; Gebbink, R. J. M. K. *Organometallics* **2008**, *27*, 2549−2559. (e) Fossey, J. S.; Russell, M. L.; Abdul Malik, K. M.; Richards, C. J. *J. Organomet. Chem.* **2007**, *692*, 4843−4848. (f) Gosiewska, S.; Martinez, S. H.; Lutz, M.; Spek, A. L.; van Koten, G.; Gebbink, R. J. M. K. *Eur. J. Inorg. Chem.*

2006, 4600−4607. (g) Wallner, O. A.; Olsson, V. J.; Eriksson, L.; Szabo, K. J. *Inorg. Chim. Acta* **2006**, *359*, 1767−1772.
(10) (a) Zhang, B.-S.; Wang, W.; Shao, D.-D.; Hao, X.-Q.; Gong, J.-F.; Song, M. P. *Organometallics* **2010**, *29*, 2579−2587. (b) Felluga, F.; Baratta, W.; Fanfoni, L.; Pitacco, G.; Rigo, P.; Benedetti, F. *J. Org. Chem.* **2009**, *74*, 3547−3550.
(11) (a) Boronat, M.; Corma, A.; Gonzalez-Arellano, C.; Iglesias, M.; Sanchez, F. *Organometallics* **2010**, *29*, 134−141. (b) Baratta, W.; Chelucci, G.; Magnolia, S.; Siega, K.; Rigo, P. *Chem.—Eur. J.* **2009**, *15*, 726−732. (c) Baratta, W.; Benedetti, F.; Del Zotto, A.; Fanfoni, L.; Felluga, F.; Magnolia, S.; Putignano, E.; Rigo, P. *Organometallics* **2010**, *29*, 3563−3570. (d) Baratta, W.; Ballico, M.; Chelucci, G.; Siega, K.; Rigo, P. *Angew. Chem., Int. Ed.* **2008**, *47*, 4362−4365.
(12) Moulton, C. J.; Shaw, B. L. *Dalton Trans.* **1976**, 1020−1024.
(13) Zargarian, D.; Castonguay, A.; Spasyuk, D. M. *Top. Organomet. Chem.* **2013**, *40*, 131−174.
(14) Wang, Z.-X.; Liu, N. *Eur. J. Inorg. Chem.* **2012**, 901−911.
(15) (a) Scok, Z.; Vechorkin, O.; Harkins, S. B.; Scopelliti, R.; Hu, X. L. *J. Am. Chem. Soc.* **2008**, *130*, 8156−8157. (b) Liang, L.-C.; Chien, P.-S.; Huang, Y.-L. *J. Am. Chem. Soc.* **2006**, *128*, 15562−15563. (c) Zhang, C.; Wang, Z.-X. *Organometallics* **2009**, *28*, 6507−6514. (d) Phapale, V. B.; Buñuel, E.; García-Iglesias, M.; Cárdenas, D. J. *Angew. Chem., Int. Ed.* **2007**, *46*, 8790−8795.
(16) Nishiyama, H. *Chem. Soc. Rev.* **2007**, *36*, 1133−1141.
(17) Monfette, S.; Turner, Z. R.; Semproni, S. P.; Chirik, P. J. *J. Am. Chem. Soc.* **2012**, *134*, 4561−4564.
(18) Pfaltz, A.; Drury, W. J., III *Proc. Natl. Acad. Sci. U.S.A.* **2004**, *101*, 5723−5726.
(19) Gelman, D.; Musa, S. *ACS Catal.* **2012**, *2*, 2456−2466.
(20) (a) Binda, P. I.; Abbina, S.; Du, G. *Synthesis* **2011**, 2609−2618. (b) Abbina, S.; Du, G. *Organometallics* **2012**, *31*, 7394−7403.
(21) (a) Shafir, A.; Buchwald, S. L. *J. Am. Chem. Soc.* **2006**, *128*, 8742−8743. (b) Kwong, F. Y.; Buchwald, S. L. *Org. Lett.* **2003**, *5*, 793−796.
(22) See Supporting Information for more details.
(23) (a) Langer, J.; Görls, H.; Fischer, R.; Walter, D. *Organometallics* **2005**, *24*, 272−279. (b) Liang, L.-C.; Chien, P.-S.; Lee, P.-Y. *Organometallics* **2008**, *27*, 3082−3093.
(24) Carmona, E.; Gonzalez, F.; Poveda, M. L.; Atwood, J. L.; Rogers, R. D. *J. Chem. Soc., Dalton Trans.* **1980**, 2108−2116.
(25) Gwynne, E. A.; Stephan, D. W. *Organometallics* **2011**, *30*, 4128−4135.
(26) (a) Ito, J.-I.; Ujiie, S.; Nishiyama, H. *Chem. Commun.* **2008**, 1923−1925. (b) Spasyuk, D. M.; Zargarian, D.; van der Est, A. *Organometallics* **2009**, *28*, 6531−6540. (c) Zhang, B.-S.; Wang, W.; Shao, D.-D.; Hao, X.-Q.; Gong, J.-F.; Song, M. P. *Organometallics* **2010**, *29*, 2579−2587.
(27) (a) Wang, H.-Y.; Meng, X.; Jin, G. −X. *Dalton Trans.* **2006**, 2579−2585. (b) Eckert, N. A.; Bones, E. M.; Lachicotte, R. J.; Holland, P. L. *Inorg. Chem.* **2003**, *42*, 1720−1725.
(28) Pandarus, V.; Zargarian, D. *Chem. Commun.* **2007**, 978−980.
(29) (a) Firme, C. L.; Pontes, D. de L.; Antunes, O. A. C. *Chem. Phys. Lett.* **2010**, *499*, 193−198. (b) Kalamse, V.; Wadnerkar, N.; Chaudhari, A. *J. Phys. Chem. C* **2010**, *114*, 4704−4709. (c) Meylemans, H. A.; Damrauer, N. H. *Inorg. Chem.* **2009**, *48*, 11161−11175. (d) Alparone, A.; Reis, H.; Papadopoulos, M. G. *J. Phys. Chem. A* **2006**, *110*, 5909−5918. (e) Solntsev, P. V.; Dudkin, S. V.; Sabin, J. R.; Nemykin, V. N. *Organometallics* **2011**, *30*, 3037−3046. (f) Solntsev, P. V.; Spurgin, K. L.; Sabin, J. R.; Heikal, A. A.; Nemykin, V. N. *Inorg. Chem.* **2012**, *51*, 6537−6547. (g) Solntsev, P. V.; Sabin, J. R.; Dammer, S. J.; Gerasimchuk, N. N.; Nemykin, V. N. *Chem. Commun.* **2010**, 6581−6583. (h) Nemykin, V. N.; Rohde, G. T.; Barrett, C. D.; Hadt, R. G.; Sabin, J. R.; Reina, G.; Galloni, P.; Floris, B. *Inorg. Chem.* **2010**, *49*, 7497−7509. (i) Nemykin, V. N.; Hadt, R. G. *J. Phys. Chem. A* **2010**, *114*, 12062−12066. (j) Nemykin, V. N.; Kobayashi, N.; Chernii, V. Y.; Belsky, V. K. *Eur. J. Inorg. Chem.* **2001**, 733−743. (k) Nemykin, V. N.; Makarova, E. A.; Grosland, J. O.; Hadt, R. G.; Koposov, A. Y. *Inorg. Chem.* **2007**, *46*, 9591−9601. (l) Nemykin, V. N.; Maximov, A. Y.; Koposov, A. Y. *Organometallics* **2007**, *26*, 3138−3148. (m) Sabin, J. R.; Varzatskii, O. A.; Voloshin, Y. Z.; Starikova, Z. A.; Novikov, V. V.; Nemykin, V. N. *Inorg. Chem.* **2012**, *51*, 8362−8372. (n) Nitta, H.; Kawata, I. *Chem. Phys.* **2012**, *405*, 93−99. (o) Jacquemin, D.; Mennucci, B.; Adamo, C. *Phys. Chem. Chem. Phys.* **2011**, *13*, 16987−16998. (p) Solomon, E. I.; Hadt, R. G. *Coord. Chem. Rev.* **2011**, *255*, 774−789. (q) Mitsopoulou, C. A. *Coord. Chem. Rev.* **2010**, *254*, 1448−1456. (r) Moore, E. G.; Samuel, A. P. S.; Raymond, K. N. *Acc. Chem. Res.* **2009**, *42*, 542−552. (s) Vlcek, A.; Zalis, S. *Coord. Chem. Rev.* **2007**, *251*, 258−287. (t) Decker, A.; Clay, M. D.; Solomon, E. I. *J. Inorg. Biochem.* **2006**, *100*, 697−706. (u) Petrenko, T.; Kossmann, S.; Neese, F. *J. Chem. Phys.* **2011**, *134*, 054116/1−054116/14. (v) Ray, K.; DeBeer, G. S.; Solomon, E. I.; Wieghardt, K.; Neese, F. *Chem.—Eur. J.* **2007**, *13*, 2783−2797. (w) Gennari, M.; Retegan, M.; DeBeer, S.; Pecaut, J.; Neese, F.; Collomb, M.-N.; Duboc, C. *Inorg. Chem.* **2011**, *50*, 10047−10055. (x) Gennari, M.; Orio, M.; Pecaut, J.; Bothe, E.; Neese, F.; Collomb, M.-N.; Duboc, C. *Inorg. Chem.* **2011**, *50*, 3707−3716. (y) Lehnert, N.; Cornelissen, U.; Neese, F.; Ono, T.; Noguchi, Y.; Okamoto, K.-I.; Fujisawa, K. *Inorg. Chem.* **2007**, *46*, 3916−3933.
(30) (a) Chmielewski, P. J.; Szterenberg, L.; Siczek, M. *Chem.—Eur. J.* **2011**, *17*, 1009−1020. (b) Bridgeman, A. J.; Courcot, B.; Nguyen, T. *Dalton Trans.* **2012**, *41*, 5362−5367. (c) Nemykin, V. N.; Polshyna, A. E.; Makarova, E. A.; Kobayashi, N.; Lukyanets, E. A. *Chem. Commun.* **2012**, *48*, 3650−3652. (d) Yamazaki, A.; Akitsu, T. *RSC Advances* **2012**, *2*, 2975−2980. (e) Dumas, A.; Luedtke, N. W. *Chem.—Eur. J.* **2012**, *18*, 245−254. (f) Sripothongnak, S.; Ziegler, C. J.; Dahlby, M. R.; Nemykin, V. N. *Inorg. Chem.* **2011**, *50*, 6902−6909. (g) Yoshinari, N.; Igashira-Kamiyama, A.; Konno, T. *Chem.—Eur. J.* **2010**, *16*, 14247−14251. (h) Soloshonok, V. A.; Ono, T.; Ueki, H.; Vanthuyne, N.; Balaban, T. S.; Burck, J.; Fliegl, H.; Klopper, W.; Naubron, J.-V.; Bui, T. T. T. *J. Am. Chem. Soc.* **2010**, *132*, 10477−10483. (i) Van Heuvelen, K. M.; Cho, J.; Dingee, T.; Riordan, C. G.; Brunold, T. C. *Inorg. Chem.* **2010**, *49*, 6535−6544. (j) Wu, T.; Li, C.-H.; Li, Y.-Z.; Zhang, Z.-G.; You, X.-Z. *Dalton Trans.* **2010**, *39*, 3227−3232. (k) Van Heuvelen, K. M.; Kieber-Emmons, M. T.; Riordan, C. G.; Brunold, T. C. *Inorg. Chem.* **2010**, *49*, 3104−3112. (l) Kieber-Emmons, M. T.; Van Heuvelen, K. M.; Brunold, T. C.; Riordan, C. G. *J. Am. Chem. Soc.* **2009**, *131*, 440−441. (m) Peralta, G. A.; Seth, M.; Ziegler, T. *Inorg. Chem.* **2007**, *46*, 9111−9125. (n) Armstrong, D. W.; Cotton, F. A.; Petrovic, A. G.; Polavarapu, P. L.; Warnke, M. M. *Inorg. Chem.* **2007**, *46*, 1535−1537. (o) Basu, P.; Nigam, A.; Mogesa, B.; Denti, S.; Nemykin, V. N. *Inorg. Chim. Acta* **2010**, *363*, 2857−2864.
(31) Hu, H.; Gao, H.; Zhu, F.; Wu, Q. *Zhongguo Kexue: Huaxue* **2012**, *42*, 628−635.
(32) Li, J.; Tian, D.; Song, H.; Wang, C.; Zhu, X.; Cui, C.; Cheng, J.-P. *Organometallics* **2008**, *27*, 1605−1611.
(33) Zhang, D.; Jin, G.-X.; Weng, L.-H.; Wang, F. *Organometallics* **2004**, *23*, 3270−3275.
(34) (a) Wang, C.; Friedrich, S.; Younkin, T. R.; Li, R. T.; Grubbs, R. H.; Bansleben, D. A.; Day, M. W. *Organometallics* **1998**, *17*, 3149−3151. (b) Connor, E. F.; Younkin, T. R.; Henderson, J. I.; Waltman, A. W.; Grubbs, R. H. *Chem. Commun.* **2003**, 2272−2273.
(35) (a) Julia-Hernandez, F.; Arcas, A.; Bautista, D.; Vicente, J. *Organometallics* **2012**, *31*, 3736−3744. (b) Vicente, J.; Arcas, A.; Julia-Hernandez, F.; Bautista, D.; Jones, P. G. *Organometallics* **2010**, *29*, 3066−3076. (c) Pandarus, V.; Zargarian, D. *Organometallics* **2007**, *26*, 4321−4334.
(36) (a) Giri, R.; Maugel, N.; Foxman, B. M.; Yu, J.-Q. *Organometallics* **2008**, *27*, 1667−1670. (b) Mawo, R. Y.; Mustakim, S.; Young, V. G., Jr.; Hoffmann, M. R.; Smoliakova, I. P. *Organometallics* **2007**, *267*, 1801−1810. (c) Song, G.; Li, X.; Song, Z.; Zhao, J.; Zhang, H. *Chem.—Eur. J.* **2009**, *15*, 5535−5544. (d) Herrmann, W. A.; Brossmer, C.; Ofele, K. *Angew. Chem., Int. Ed.* **1995**, *34*, 1844−1848.
(37) Deeming, A. J.; Rothwell, I. P. *J. Orgnomat. Chem.* **1981**, *205*, 117−131.
(38) (a) Desimoni, G.; Faita, G.; Jørgensen, K. A. *Chem. Rev.* **2011**, *111*, PR284−PR437. (b) Desimoni, G.; Faita, G.; Jørgensen, K. A. *Chem. Rev.* **2006**, *106*, 3561−3651. (c) Hargaden, G. C.; Guiry, P. J. *Chem. Rev.* **2009**, *109*, 2505−2550.

(39) Kim, M.; Liu, Q.; Gabbaï, F. P. *Organometallics* **2004**, *23*, 5560−5564.
(40) Rothwell, I. P. *Acc. Chem. Res.* **1988**, *21*, 153−159.
(41) Perutz, R. N.; Sabo-Etienne, S. *Angew. Chem., Int. Ed.* **2007**, *46*, 2578−2592.
(42) Higgs, A. T.; Zinn, P. J.; Simmons, S. J.; Sanford, M. S. *Organometallics* **2009**, *28*, 6142−6144.
(43) Zeller, A.; Herdtweck, E.; Strassner, T. *Eur. J. Inorg. Chem.* **2003**, 1802−1806.
(44) Tomasi, J.; Mennucci, B.; Cammi, R. *Chem. Rev.* **2005**, *105*, 2999−3093.
(45) (a) Xu, X.; Goddard, W. A., III *Proc. Natl. Acad. Sci. U.S.A.* **2004**, *101*, 2673−2677. (b) Lee, C.; Yang, W.; Parr, R. G. *Phys. Rev. B* **1988**, *37*, 785−789.
(46) McLean, A. D.; Chandler, G. S. *J. Chem. Phys.* **1980**, *72*, 5639−5648.
(47) Tenderholt, A. L. *QMForge*, Version 2.1; Stanford University: Stanford, CA, U.S.A.